

# Journal of Materials Chemistry B

Accepted Manuscript



This is an *Accepted Manuscript*, which has been through the Royal Society of Chemistry peer review process and has been accepted for publication.

*Accepted Manuscripts* are published online shortly after acceptance, before technical editing, formatting and proof reading. Using this free service, authors can make their results available to the community, in citable form, before we publish the edited article. We will replace this *Accepted Manuscript* with the edited and formatted *Advance Article* as soon as it is available.

You can find more information about *Accepted Manuscripts* in the [Information for Authors](#).

Please note that technical editing may introduce minor changes to the text and/or graphics, which may alter content. The journal's standard [Terms & Conditions](#) and the [Ethical guidelines](#) still apply. In no event shall the Royal Society of Chemistry be held responsible for any errors or omissions in this *Accepted Manuscript* or any consequences arising from the use of any information it contains.

# Fabrication of polymer brush surfaces with highly-ordered perfluoroalkyl side groups at the brush end and their antibiofouling properties

*Lin Wang, Xiang Chen, Xinyu Cao, Jianquan Xu, Biao Zuo, Li Zhang, Xinping Wang\*, Juping Yang, Yanqing Yao*

Department of Chemistry, Key Laboratory of Advanced Textile Materials and Manufacturing Technology of the Education Ministry, Zhejiang Sci-Tech University, Hangzhou 310018, China

**ABSTRACT:** Acrylate block polymer brushes ( $\text{Au-PMMA}_{65}\text{-}b\text{-PODMA}_y\text{-}ec\text{-FMA}_2$ ) with two 2-perfluorooctylethyl methacrylate units at the brush end were successfully prepared on a Au substrate by a “grafting to” method. Characterization by XPS, contact angle measurement, ellipsometry and nanomechanical measurement showed that a well-ordered and perpendicularly oriented structure of the perfluoroalkyl side chains on the brush surface was enhanced with increasing degree of polymerization ( $y$ ) of poly ( $n$ -octadecyl methacrylate), and a crystalline structure of perfluoroalkyl side chains formed when  $y$  was equal to 24. Protein adsorption studies indicated that the adsorbed mass of fibrinogen decreased with increasing order of the structure of the perfluoroalkyl side chains at the brush end. When the perfluoroalkyl group on the brush surface formed a crystal structure, there was only trace fibrinogen adsorption on the brush surface. This work demonstrates that the protein-resistant performance was enhanced greatly by constructing polymer brush surfaces with well-ordered and perpendicularly oriented structures of the perfluoroalkyl side chains.

**Keywords:** polymer brush, end-capped brush, fluorinated brush, surface structure, protein adsorption

## 1. INTRODUCTION

Materials with antibiofouling surfaces, which resist the nonspecific adsorption of proteins, cells, or other biological species, are important for a wide variety of applications, ranging from surgical equipment,<sup>1,2</sup> medical implants,<sup>3,4</sup> food packaging<sup>5</sup> and storage,<sup>6</sup> textiles,<sup>7,8</sup> biosensors,<sup>9</sup> and water purification systems,<sup>10</sup> as well as marine applications such as the coating of ship hulls.<sup>11,12</sup> Thus, a polymer surface which has excellent antibiofouling properties attract considerable practical and theoretical interest.<sup>13-15</sup> Currently, hydrophilic coatings are among the most popular antibiofouling materials in use. It is well-accepted that the hydration layer formed at the interface of this kind of coatings should resist nonspecific protein adsorption.<sup>16,17</sup> Film surfaces with a 25-45 nm thick poly (hydroxypropyl methacrylate) and poly(2-hydroxyethyl methacrylate) layer can achieve almost zero protein adsorption ( $<0.3 \text{ ng/cm}^2$ ) from single-protein solution and diluted human blood plasma and serum.<sup>18</sup> However, their super low-fouling ability may be lost due to oxidative damage in most biochemically relevant solutions.<sup>19,20</sup> When this occurs, foulants could penetrate the hydration layer, firmly attaching to the hydrophilic surfaces and thus destroy the antifouling effect.<sup>21</sup>

Conversely, according to theory of adhesion,<sup>22,23</sup> it is assumed that the release property of a material is primarily determined by its surface free energy, ultimately giving rise to water repellency. To reduce biofouling, hydrophobic coatings fluorocarbons were investigated widely due to their low surface energy.<sup>24-28</sup> The lowest surface tension ( $6 \text{ mJ/m}^2$ ) would be obtained when trifluoromethyl ( $-\text{CF}_3$ ) groups was closely packed on the material surface.<sup>29</sup> It was reported<sup>30</sup> that cured fluorinated polyimides suppressed protein adsorption because of their low surface free energy. However, the overall performance of fluorocarbon-based coatings has, to date, been disappointing.<sup>14</sup> Some results showed<sup>25,26,31-33</sup> that the hydrophobic fluorinated surfaces were, in fact, not resistant to protein adsorption.

It was reported that the fluorinated polymer surfaces do not always exhibit enrichment of fluorine components and their surface structure which determine their

surface free energy,<sup>34</sup> to a great extent, depends on many factors such as the chemical structure of the polymer,<sup>35-38</sup> film-formation methods<sup>39-42</sup> and conditions.<sup>37,43</sup> The surface enrichment of the fluorine component of films prepared by the spin-coating technique is much lower than that of those prepared by the casting technique or by melting of polymer grains onto the substrate.<sup>37, 40</sup> The spin-coated films of poly(methyl methacrylate)-*b*-poly(2-perfluorooctylethyl methacrylate) diblock copolymer formed a micelle structure with a PFMA core and PMMA shell, resulting in an absence of any fluorine component near the surface.<sup>42</sup> It is well known that protein resistance is ultimately determined by the outermost surface structure.<sup>44</sup> Therefore, the various factors described above might contribute to the argument concerning whether or not fluorinated materials can resist protein adsorption. At the same time, polymer usually reconstructs at their surface and loses their low-energy surface properties when exposed to polar liquids.<sup>45</sup> Several reports have demonstrated that surface reconstruction under water is the main reason for the loss of the protein-resistant performance of fluorinated polymers.<sup>34,46,47</sup> An effective approach to prevent surface reconstruction from occurring is to induce uniform CF<sub>3</sub> surfaces to form liquid crystalline (LC) phases that would effectively “freeze” the surface structure.<sup>45</sup>

To consider the goal of creating a low-energy release surface through the incorporation of low surface-tension functional groups into a polymer chain, the optimal polymer architecture suggested for achieving this goal included both high- and low-energy functional groups placed at two ends of the polymer chain. Such an arrangement has been termed a “push-me/pull-you” structure.<sup>48</sup> This type of structure has been shown to be favorable toward low-surface-tension moieties self-assembling on the polymer surface during film formation, resulting in better chain alignment and packing of the low surface-tension moieties. Polymer brushes with a hydrophobic group at the brush end are typical push-me/pull-you structures, providing an exemplary system of materials to achieve ultrathin hydrophobic coatings with well-defined surface structures. Cho et al.<sup>49</sup> demonstrated that the degree of octadecyltrichlorosilane (OTS) molecular ordering was of great significance in

regulating the corresponding adhesion and adsorption behaviors. They found that bovine serum albumin (BSA) and human fibrinogen (HF) adhered more strongly to the disordered, rather than to the ordered, OTS monolayer.

In this paper, we designed fluorinated units end-capped diblock copolymers poly(methylmethacrylate)-*b*-poly(*n*-octadecylmethacrylate)-*ec*-poly(2-perfluorooctylethyl methacrylate) (FMA-*ec*-PODMA-*b*-PMMA-S)<sub>2</sub> with a disulfide group in the chain center by atom transfer radical polymerization(ATRP), and then used a “grafting to” method to graft the fluorinated polymer on to a gold substrate. Ordered structures on the fluorinated polymer brush surfaces were prepared and their protein adsorption behavior was investigated.

## 2. EXPERIMENTAL SECTION

### 2.1 Materials

Methyl methacrylate (MMA) (Shanghai Reagent Co. , China) and 2-perfluorooctylethyl methacrylate (FMA) (Aldrich Chemical Co., USA) were washed with 5 wt% NaOH aqueous solution and deionized water, dried through CaH<sub>2</sub>, and then vacuum-distilled before polymerization. *n*-Octadecyl methacrylate (ODMA) (Polysciences Inc.; 99%) was purified by dissolving in hexane and then extracted four times with 5% aqueous NaOH. After the organic phase was dried over magnesium sulfate, the solution was passed through neutral alumina, and solvent was removed under reduced pressure.<sup>50</sup> CuBr (5 g) was stirred in glacial acetic acid (100 mL) overnight. The content was filtered through a Buchner funnel and washed three times with ethanol and diethyl ether, dried in a vacuum overnight, and stored under nitrogen.<sup>51</sup> *N,N,N',N'',N''*-pentamethyl-diethylenetriamine (PMDETA), 11-mercapto-1 -undecanol, and 2-bromoisobutyryl bromide were purchased from Aldrich Chemical Co., and used as received. Toluene was purified in the usual manner and dried by refluxing over sodium and distilled prior to use. Fluorescein isothiocyanate-labeled bovine serum albumin (FITC-BSA) was purchased from Wanhuaishi Biotech Co. (Beijing, China). Human plasma fibrinogen was purchased

from Shanghai Jianglai Co. (Shanghai, China). Phosphate-buffered saline solution (PBS, 0.1 M, pH 7.4) was prepared according to previously published methods.<sup>52</sup> Other reagent grade chemicals were purchased from Shanghai Reagent Co. and used without further purification.

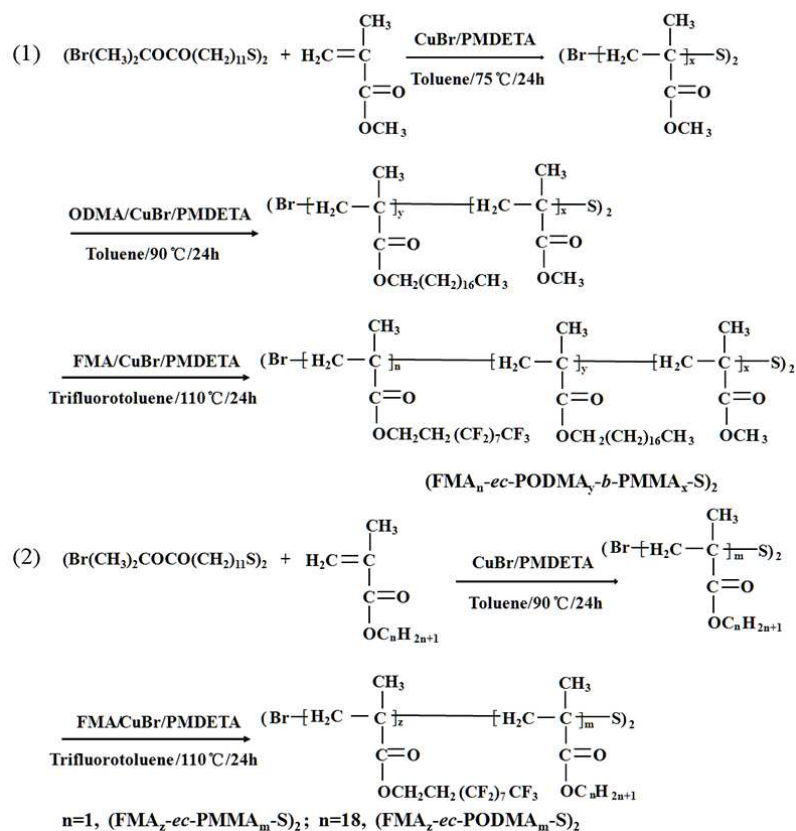
## 2.2 Preparation of fluorinated acrylate copolymers by ATRP

*Synthesis of initiator (BrC(CH<sub>3</sub>)<sub>2</sub>COO(CH<sub>2</sub>)<sub>11</sub>S)<sub>2</sub>.* (BrC(CH<sub>3</sub>)<sub>2</sub>COO(CH<sub>2</sub>)<sub>11</sub>S)<sub>2</sub> was synthesized according to the reported method.<sup>53,54</sup> Dichloromethane (150 mL), 10% potassium hydrogen carbonate (20 mL), and 11-Mercapto-1-undecanol (4.06 g,) were added to a round-bottom flask. A solution of bromine (10 mmol, 1.6 g) was added dropwise to the well-stirred mixture at room temperature. The color of the bromine quickly disappeared upon addition to the flask. The organic phase was then separated from the solution, and the aqueous phase was extracted with dichloromethane. The organic phases were subsequently combined and dried with MgSO<sub>4</sub>. All solvent was removed by rotary evaporation, and highly pure disulfide (HO(CH<sub>2</sub>)<sub>11</sub>S)<sub>2</sub> was obtained, as confirmed by <sup>1</sup>H NMR, with the resulting spectrum identical to a previously reported spectrum.<sup>55</sup>

2-bromoisobutyryl bromide (1.80 mL, 14.8 mmol) was added drop by drop to a stirred solution of (HO(CH<sub>2</sub>)<sub>11</sub>S)<sub>2</sub> (2.5 g) and triethylamine (4.2 mL) in 150 mL dry dichloromethane at 0 °C under a nitrogen atmosphere. The solution was stirred for 1 h at 0 °C and then at 25°C for another 2 h to complete the reaction. Triethylamine hydrobromide was filtered off, and the solution was extracted with aqueous 2 M Na<sub>2</sub>CO<sub>3</sub> saturated with NH<sub>4</sub>Cl. The organic phase was collected and dried over MgSO<sub>4</sub>, and volatiles were evaporated under reduced pressure. The crude product was purified by column chromatography, resulting in a viscous, pale yellow liquid (BrC(CH<sub>3</sub>)<sub>2</sub>COO (CH<sub>2</sub>)<sub>11</sub>S)<sub>2</sub>. The structure of the resulting product was confirmed by <sup>1</sup>H NMR, <sup>13</sup>C NMR and element analysis, and was the same as previously reported in Ref [55,56].

*Synthesis of fluorinated diblock copolymers of poly(methyl methacrylate)-b-poly (n-octadecyl methacrylate) end-capped with 2-perfluoro octylethyl methacrylate (FMA<sub>2</sub>-ec-PODMA<sub>y</sub>-b-PMMA<sub>65</sub>-S-S-PMMA<sub>65</sub>-b-PODMA<sub>y</sub>*

-*ec-FMA*<sub>2</sub>). The preparation of *FMA*<sub>2</sub>-*ec-PODMA*<sub>y</sub>-*b-PMMA*<sub>65</sub>-*S-S-PMMA*<sub>65</sub>-*b-PODMA*<sub>y</sub>-*ec-FMA*<sub>2</sub> by atom-transfer radical polymerization (ATRP) is outlined in Scheme 1. In the first step, macroinitiator (Br-PMMA<sub>65</sub>-S)<sub>2</sub> was prepared in a three-neck round-bottom flask equipped with a Teflon-coated magnetic stir. Prior to



Scheme 1. Procedure for synthesis of fluorinated acrylate copolymers.

use, the flask was vacuumed and back-filled with dry nitrogen three times. Methyl methacrylate (MMA), *N,N',N'',N''*-pentamethyl-diethylenetriamine (PMDETA), CuBr and initiator synthesized above were added sequentially under a nitrogen atmosphere with the molar ratio of [MMA] / [PMDETA] / [CuBr] / [Initiator] of 100 : 2 : 1 : 1 into toluene to give a reaction solution. The polymerization was carried out at 70°C under a nitrogen atmosphere for 24 h. The polymerization was then stopped by cooling to room temperature and opening the flask to air. The mixture was passed

through a neutral alumina column, the solution was precipitated into methanol, and the resulting product was filtered and dried under vacuum. The molecular weight of the macroinitiator was determined to be 13000 by gel permeation chromatography (GPC), namely (Br-PMMA<sub>65</sub>-S)<sub>2</sub>.

*Br-PODMA<sub>y</sub>-b-PMMA<sub>65</sub>-S-S-PMMA<sub>65</sub>-b-PODMA<sub>y</sub>-Br* diblock copolymers were prepared in a Florence flask containing a magnetic stirring bar. After the macroinitiator (Br-PMMA<sub>65</sub>-S)<sub>2</sub>, CuBr and PMDETA were introduced into the flask, the flask was vacuumed and back-filled with dry nitrogen several times, prior to the addition of toluene. Once the solution became homogeneous, *n*-octadecyl methacrylate (ODMA) was added to the flask, with the following molar ratios: (Br-PMMA<sub>65</sub>-S)<sub>2</sub> / [CuBr]/[PMDETA]/[ODMA] of 1:1:2:10, 1:1:2:25, 1:1:2:40 or 1:1:2:60. Following this step, polymerization was performed at 90°C under a nitrogen blanket for 24 h. After polymerization, the mixture was diluted with THF and passed through an Al<sub>2</sub>O<sub>3</sub> column. The resulting solution was filtered and then precipitated into methanol. The resulting polymer was dried under vacuum at room temperature.

*FMA<sub>2</sub>-ec-PODMA<sub>y</sub>-b-PMMA<sub>65</sub>-S-S-PMMA<sub>65</sub>-b-PODMA<sub>y</sub>-ec-FMA<sub>2</sub>* polymers were synthesized by ATRP with *Br-PODMA<sub>y</sub>-b-PMMA<sub>65</sub>-S-S-PMMA<sub>65</sub>-b-PODMA<sub>y</sub>-Br* as the macroinitiator. First, the macroinitiator, CuBr, and PMDETA were introduced into the flask, and the flask was vacuumed and back-filled with dry nitrogen several times. Benzotrifluoride was then added to the flask. Once the solution became homogeneous, 2-perfluorooctylethyl methacrylate (FMA) was added into the solution with the molar ratios of [(*Br-PODMA<sub>y</sub>-b-PMMA<sub>65</sub>-S*)<sub>2</sub>]/[CuBr]/[PMDETA]/[FMA] of 1:1:2:3. Polymerization was performed at 110°C under a nitrogen blanket for 10 h. After polymerization, the mixture was diluted with THF and passed through an alumina column. The reaction solution was filtered and then precipitated into methanol. The resulting product was dried under vacuum at room temperature. The chemical structures and characteristics of the various polymer products are shown in Table 1.

*Synthesis of other polymers end-capped with 2-perfluorooctylethyl methacrylate.* (FMA<sub>2</sub>-ec-PMMA<sub>65</sub>-S)<sub>2</sub>, (FMA<sub>y</sub>-ec-PMMA<sub>126</sub>-S)<sub>2</sub> and (FMA<sub>2</sub>-ec-PODM<sub>103</sub>-S)<sub>2</sub> were prepared using the aforementioned method.<sup>57,58</sup> The characteristics of these polymers

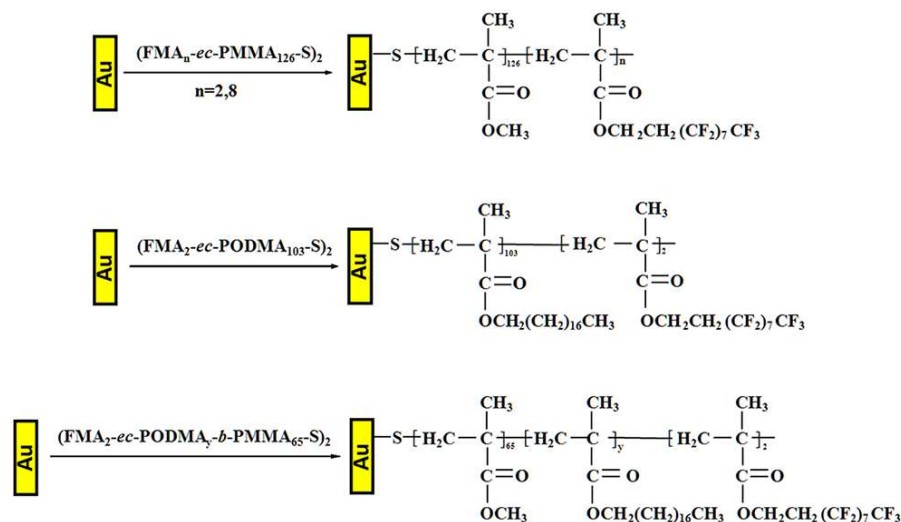
are listed in Table 1.

In order to confirm the structures of polymers with a disulfide group, the tributylphosphine ( $\text{Bu}_3\text{P}$ ) was used, as in a previously reported method,<sup>59</sup> to cleave the polymethacrylates with a disulfide group, converting them to thiol-terminated polymers. To perform this reaction, 0.08g  $(\text{Br-PMMA}_{126}\text{-S})_2$  was dissolved in 5mL THF, and 0.1mL  $\text{Bu}_3\text{P}$  was added. The degradation was almost complete within 20 h at room temperature. The molecular weights of the most products were approximately half that of  $(\text{Br-PMMA}_{126}\text{-S})_2$  as shown in Fig.S1 (ESI†), which indicates that the disulfide link was in the middle of the polymer chains. The shoulder peak in GPC trace of thiol-terminated polymers corresponds few polymer which was not cleaved, which molecular weight was same as that of  $(\text{Br-PMMA}_{126}\text{-S})_2$ .

### 2.3. Preparation of fluorinated acrylate copolymer grafted Au surfaces

Glass slides (10mm×10mm) were cleaned in piranha solution at 50°C for 3 h. The slides were then rinsed thoroughly in deionized water, ethanol and methanol and dried under a stream of nitrogen. (Caution: Piranha solution reacts violently with many organic materials and should be handled with extreme care.) The clean slides were stored in an oven at 110°C. Thin layers of nickel (20 nm) and gold (120 nm) were then successively deposited onto dry substrates by physical vapor deposition.<sup>60</sup> A 20 nm thick layer of nickel was used to promote adhesion between the glass and the gold film.

The polymers were dissolved in toluene or trifluorotoluene (trifluorotoluene was used for fluorinated polymers) to make a 0.2 % polymer solution, and the solutions were filtered through a porous PTFE filter (with pore size of 0.25  $\mu\text{m}$  in diameter). The preparation of fluorinated polymer brushes on gold substrate is illustrated in Scheme 2. The polymer brushes were formed on the surface of the gold substrate by immersing the substrate into 0.2 % solution of the polymer, using as solvent either toluene or trifluorotoluene at room temperature. The time used to form each polymer brush is indicated together with the results for each experiment. After formation, each polymer brush was rinsed sequentially in copious amounts of toluene and ethanol, and then dried in vacuum at 80°C for 24 h.



Scheme 2. Schematic for formation of fluorinated polymer brushes on the surface of gold substrate.

#### 2.4. Characterization

The molecular weights of the polymers were determined by gel permeation chromatography (GPC) using a Waters 1515 Isocratic HPLC Pump and Waters 2414 Refractive Index Detector with tetrahydrofuran (THF) as the eluent at 35 °C, at a flow rate of 1.0 ml/min. The GPC chromatograms were calibrated against poly(methyl methacrylate) standards. <sup>1</sup>H NMR spectra were recorded on a Bruker Avance AMX-400 NMR instrument in CDCl<sub>3</sub> with tetramethylsilane (TMS) as an internal standard. The FT-IR spectra of the copolymers were measured on a Nicolet Avatar 370 Fourier Transform Infrared (FT-IR) spectrometer. The fluorine contents of the fluorinated acrylate copolymers were obtained through fluorine elemental analysis using the ignition method.

Contact angles ( $\theta$ ) of water and oil on the surfaces were conducted using a DSA10-MK2 drop shape analysis system (Krüss Co., Germany) at 25°C. The volume of the liquid drops used was 3  $\mu$ L. The reported  $\theta$  values were the averages of at least five samples, which eight measurements were taken for every sample within 10-20 seconds of applying each drop of liquid. The surface free energies were calculated

according to Owens and Wendt's theory<sup>61</sup> from the measured contact angles of water and diiodomethane on the samples. The experimental errors for measuring the  $\theta$  values were evaluated to be less than  $\pm 2^\circ$ , thus indicating that the results were sufficiently accurate. X-ray photoelectron spectroscopy (XPS) was performed using a PHI-5000C ESCA System with an Mg K $\alpha$  X-ray source (1253.6eV). The X-ray gun was operated at a power of 250 W and the high voltage was maintained at 140 kV with a detection angle of  $30^\circ$ . The chamber pressure during analysis was about  $1 \times 10^{-8}$  Torr. All spectra were calibrated using the C<sub>1s</sub> peak of the C-C bond at 284.6 eV. Ellipsometry measurements were performed on an ellipsometer (Accurion Co., Germany) at a fixed angle of incidence of  $60^\circ$ . For the thickness layer calculations, refractive indices of  $n=1.49$  were used for the polymers.

Nanomechanical measurements were performed using the PeakForce QNM (Quantitative Nano-Mechanics) mode on a Bruker MultiMode 8 AFM instrument at various temperatures. This mode is far more advanced than previous modes, as noted by its ease of operation, fast scanning speed and capability of simultaneously providing both high resolution morphological images<sup>62</sup> and accurate quantitative mechanical information.<sup>63,64</sup> Surface deformation, the maximum adhesive force between tip and sample ( $F_{adh}$ ), dissipation energy and elastic modulus can all be acquired from the resulting force curve. The nanomechanical properties can be extracted from the force curve, from which the elastic modulus of the samples can be obtained by fitting the Derjaguin–Muller–Toporov (DMT) Model<sup>65,66</sup> to the part of the force curve where the sample and tip are in contact, as given by the equation:

$$F = \frac{4}{3} E^* \sqrt{Rd^3} + F_{adh}$$

Here,  $F$  is the force,  $E^*$  is the effective elastic modulus,  $R$  is the tip radius,  $d$  is the deformation value at a given force, and  $F_{adh}$  the maximum adhesion force. In this study, the tip radius was determined by an indirect method where the radius was adjusted to achieve the correct value of a sample with known elastic modulus (polystyrene,  $E = 2.7$  GPa).

Force-displacement curves were acquired at different temperatures by heating the

base of the brush samples through a heating stage system provided by Bruker Nano Inc., which has a unique high temperature distortionless imaging technology that can adjust the temperature from -35 °C to 250°C, with accuracy of  $\pm 1$ K. The temperature of the heating stage was calibrated by a standard sample. For each temperature, the sample was heated for 2h, so that it could reach an equilibrium temperature. Each experiment was repeated at least five times, using a fresh polymer brush each time, to ensure the reproducibility of results. The reported values were the averages of at least four samples.

### 2.5. Protein adsorption

The different specimens were incubated with 0.1 mg/ml protein (fibrinogen or FITC-BSA) in PBS buffer (PH=7.4) at room temperature. After 60min, the specimens were removed from the protein solution, washed thoroughly with PBS buffer, followed by rinsing with deionized water and dried in a stream of nitrogen gas.

FITC-BSA adsorption measurements were examined by fluorescence microscopy (Olympus, Japan). Fibrinogen adsorption measurements of these samples were then performed by X-ray photoelectron spectroscopy (XPS). Fibrinogen adsorption was calculated by integration of the peak area of the  $N_{1s}$  peak from the corresponding XPS spectrum.

## 3. RESULTS AND DISCUSSION

### 3.1 Synthesis and characterization of end-capped polymethacrylates with center disulfide bond

A bifunctional initiator ( $\text{BrC}(\text{CH}_3)_2\text{COO}(\text{CH}_2)_{11}\text{S}_2$ ) was used to prepare end-capped polymethacrylates with a disulfide bond in the center via a step-by-step ATRP technique. The poly (methyl methacrylates) or poly (*n*-octadecyl methacrylate) end-capped with several FMA units (*n*), ( $\text{FMA}_n\text{-}ec\text{-PMMA}_x\text{-S-S-PMMA}_x\text{-}ec\text{-FMA}_n$  or  $\text{FMA}_n\text{-}ec\text{-PODMA}_{103}\text{-S-S-PODMA}_{103}\text{-}ec\text{-FMA}_n$ ), were prepared by ATRP using the corresponding macroinitiators  $\text{Br-PMMA}_x\text{-S-S-PMMA}_x\text{-Br}$  ( $x=65, 126$ ) or  $\text{Br-PODMA}_{103}\text{-S-S-PODMA}_{103}\text{-Br}$ , respectively. The targeted numbers of FMA units

(i.e. the  $n$  values) were an average of either two or eight.

The Br-PODMA $_y$ -*b*-PMMA $_{65}$ -S-S-PMMA $_{65}$ -*b*-PODMA $_y$ -Br triblock copolymer was synthesized by Br-PMMA $_{65}$ -S-S-PMMA $_{65}$ -Br macroinitiator. Fig.S2 (ESI†) and Fig.S3 (ESI†) show representative GPC trace and  $^1\text{H}$  NMR spectra of both (Br-PMMA $_{65}$ -S) $_2$  and (Br-PODMA $_y$ -*b*-PMMA $_{65}$ -S) $_2$ . Since the degree of polymerization of the methyl methacrylate block is known from GPC analysis prior to the second polymerization, the block ratio can be calculated from the integrated intensity ratio of the peak at 3.60 ppm to the peak at 3.90 ppm, which are attributed to  $-\text{OCH}_3$  relative to the MMA unit and  $-\text{OCH}_2(\text{CH}_2)_{16}\text{CH}_3$ , relative to the ODMA unit,<sup>67</sup> respectively. The Br-PODMA $_y$ -*b*-PMMA $_{65}$ -S-S-PMMA $_{65}$ -*b*-PODMA $_y$ -Br with various degrees of polymerization ( $y$ ) was estimated in the same way, and the results are given in Table 1.

Table 1. Characteristics of all end-capped polyacrylates used in this study

Samples	$M_n \times 10^{-4}$ <sup>a,b</sup>	$W_F(\%)$ <sup>c</sup>	FMA (mol%) <sup>d</sup>
(FMA $_2$ - <i>ec</i> -PMMA $_{65}$ -S) $_2$	1.5	8.39	2.93
(FMA $_2$ - <i>ec</i> -PMMA $_{126}$ -S) $_2$	2.8	5.36	1.83
(FMA $_8$ - <i>ec</i> -PMMA $_{126}$ -S) $_2$	3.4	14.88	5.94
(FMA $_2$ - <i>ec</i> -PODMA $_{103}$ -S) $_2$	7.2	1.85	1.95
(FMA $_2$ - <i>ec</i> -PODMA $_6$ - <i>b</i> -PMMA $_{65}$ -S) $_2$	1.8	5.23	2.10
(FMA $_2$ - <i>ec</i> -PODMA $_{13}$ - <i>b</i> -PMMA $_{65}$ -S) $_2$	2.3	4.43	2.10
(FMA $_2$ - <i>ec</i> -PODMA $_{19}$ - <i>b</i> -PMMA $_{65}$ -S) $_2$	2.7	3.64	1.83
(FMA $_2$ - <i>ec</i> -PODMA $_{24}$ - <i>b</i> -PMMA $_{65}$ -S) $_2$	3.1	3.44	1.88

- a) Determined by GPC, and calibrated by poly(methyl methacrylate) standards. b) Calculated from  $^1\text{H}$  NMR and elemental analysis. c)  $W_F(\%)$  represents fluorine content obtained from fluorine elemental analysis. d) FMA (mol%) represents fluorine monomer content obtained from fluorine elemental analysis.

The triblock copolymers, Br-PODMA<sub>y</sub>-*b*-PMMA<sub>65</sub>-S-S-PMMA<sub>65</sub>-*b*-PODMA<sub>y</sub>-Br, were chain extended with 2-perfluorooctylethyl methacrylate (FMA) units using the CuBr/PMDETA catalytic reaction system in benzotrifluoride at 110°C to produce the FMA end-capped copolymers FMA<sub>n</sub>-*ec*-PODMA<sub>y</sub>-*b*-PMMA<sub>65</sub>-S-S-PMMA<sub>65</sub>-*b*-PODMA<sub>y</sub>-*ec*-FMA<sub>n</sub>. The FMA content was controlled to be two units at the triblock copolymer chain end. At such low FMA concentrations, the molecular weight difference between the macro-initiator and the resulting fluorinated polymer was too low to be detectable by either GPC or by <sup>1</sup>H NMR. Consequently, fluorine elemental analysis was employed to determine the fluorinated monomer content.<sup>68</sup> The amount of FMA units (*n*) in the end-capped polymers was calculated according to following equation:

$$W_F (\%) = (17 \times 19 \times n) / (M_n + 532 \times n).$$

where  $W_F$  is the fluorine content,  $M_n$  is the molecular weight of the macroinitiator and  $n$  is the number of FMA units, which is also the polymerization degree of PFMA. The molecular weight of fluorinated monomer FMA is 532. Table 1 shows the chemical structures of all end-capped polymers used in this study. The incorporation of FMA units in the copolymers can be substantiated by FT-IR, as shown in Fig.S4 (ESI†). Compared with the macroinitiator, a new absorbance at about 660 cm<sup>-1</sup> appeared in the spectra of the fluorinated polymers which was attributed to the rocking and wagging vibrations of CF<sub>2</sub> groups, indicating the incorporation of the FMA blocks.<sup>69</sup>

### 3.2. Characterization of Polymer-Grafted Gold Surfaces

Recently, Duwez showed<sup>70,71</sup> that the transformation of dithioesters and trithiocarbonates into thiols or disulfides was not mandatory for the functionalization of metal surfaces, as these two species are able to chemisorb onto gold with a grafting density close to that obtained with thiols. Motivated by these encouraging results, we attempted to fabricate thick brushes consisting of a diblock copolymer end-capped with fluorinated units on a planar surface of gold, in which two sulfur atoms exist as a disulfide bond in the polymer center, interacting with the gold substrate. After soaking in 0.2% polymer trifluorotoluene (or toluene) solution, the gold surface was washed in copious amounts of trifluorotoluene (or toluene) in order to remove physically

adsorbed polymer, leaving only the covalently immobilized fluorinated polyacrylate brush (shown in Fig.S5 (ESI<sup>†</sup>)). The growth of the brush on the planar gold surface was confirmed and thoroughly documented by XPS, water contact angle measurement and ellipsometry.

The growth of the diblock polyacrylate end-capped with fluorinated unit brush was traced by ellipsometry and water contact angle as shown in Fig.1. It is obvious that both the thickness of the fluorinated polyacrylate brush layer and the water contact angle increased very rapidly with increasing deposition time. After 24h, the thickness of the resulting fluorinated polymer brush was about  $20\pm 2$ nm, and the water contact angle eventually increased to  $125^\circ$ . The thicknesses of these brushes were similar to some reported value of V-shaped brush,<sup>72</sup> but seem to be larger than that prepared by a typical grafting-to method as most reported. The reason may be attributed to the crystallinity of the long alkyl chain side group in these block copolymer brushes. This surface was analyzed by XPS and the results given in Fig.S6 (ESI<sup>†</sup>) show that the characteristic peaks of Au nearly disappeared, indicating that the fluorinated polymer brush provided full coverage on the gold surface.

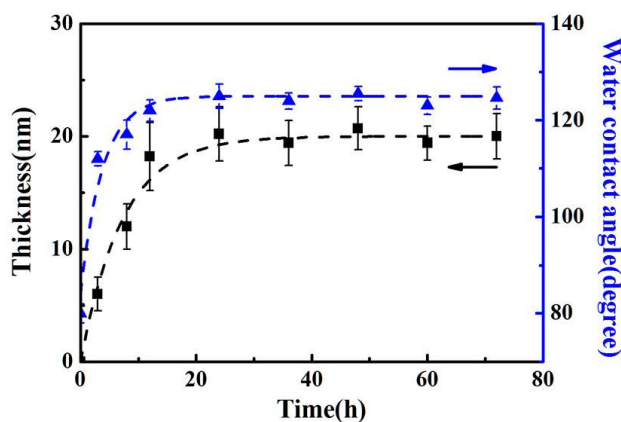


Fig.1 Deposition time dependence of Au-PMMA<sub>65</sub>-*b*-PODMA<sub>24</sub>-*ec*-FMA<sub>2</sub> brush thickness and water contact angle. 0.2 % FMA<sub>2</sub>-*ec*-PODMA<sub>24</sub>-*b*-PMMA<sub>65</sub>-S-S-PMMA<sub>65</sub>-*b*-PODMA<sub>24</sub>-*ec*-FMA<sub>2</sub> trifluorotoluene solution, T=25°C

In order to investigate the effect of the structures of the fluorinated polymer brushes on their corresponding surface properties, the surface properties of Au-PMMA<sub>126-ec-FMA</sub><sub>2</sub>, Au-PODMA<sub>103-ec-FMA</sub><sub>2</sub> and Au-PMMA<sub>65-b-PODMA</sub><sub>24-ec-FMA</sub><sub>2</sub> brushes are shown in Table 2. It is apparent that the presence of only two FMA units at the brush end is sufficient to increase the contact angles of water and paraffin oil. The contact angles of water of Au-PMMA<sub>126-ec-FMA</sub><sub>2</sub> and

Table 2. Surface properties of Au-PMMA<sub>126-ec-FMA</sub><sub>2</sub>, Au-PODMA<sub>103-ec-FMA</sub><sub>2</sub>, and Au-PMMA<sub>65-b-PODMA</sub><sub>24-ec-FMA</sub><sub>2</sub> brushes

Sample	Thickness (nm)	Contact angle (degree)		Surface energy (mJ/m <sup>2</sup> )	F/C ratio
		water	oil		
Au-PMMA <sub>126-ec-FMA</sub> <sub>2</sub>	20.0±2.3	113±1	68±2	15.54	0.69
Au-PODMA <sub>103-ec-FMA</sub> <sub>2</sub>	24.1±1.5	118±1	72±2	10.92	0.91
Au-PMMA <sub>65-b-PODMA</sub> <sub>24-ec-FMA</sub> <sub>2</sub>	20.2±2.0	125±1	87±2	8.07	1.18

Au-PODMA<sub>103-ec-FMA</sub><sub>2</sub> reached 113° and 118°, respectively, which are the close to that the value of poly(2-perfluorooctylethyl methacrylate) homopolymer (PFMA) (120°).<sup>35,73</sup> Similar results were observed for the contact angles of paraffin oil on the surface of Au-PMMA<sub>126-ec-FMA</sub><sub>2</sub> and Au-PODMA<sub>103-ec-FMA</sub><sub>2</sub>. The contact angles of water and paraffin oil of Au-PMMA<sub>65-b-PODMA</sub><sub>24-ec-FMA</sub><sub>2</sub> reached 125° and 87° respectively. The surface free energies and F/C ratios of these fluorinated polymer brushes determined from XPS are in agreement with the results of the contact angle measurements. These results are similar to those of the corresponding solution-cast film.<sup>38,39</sup>

In general, fluorinated copolymers usually lose their low-energy surface properties because of molecular rearrangement when the surface is exposed to polar liquids.<sup>34,38,45</sup> To investigate the resistance to surface reconstruction of the above three series of fluorinated polymer brushes, the water contact angle measurements were performed after immersing in water at 25 °C for different times. For the results, as shown in Fig. 2, the water contact angle of the Au-PMMA<sub>65-b-PODMA</sub><sub>24-</sub>

*ec*-FMA<sub>2</sub> surface only decreased 7°, much smaller than the 17° obtained for the

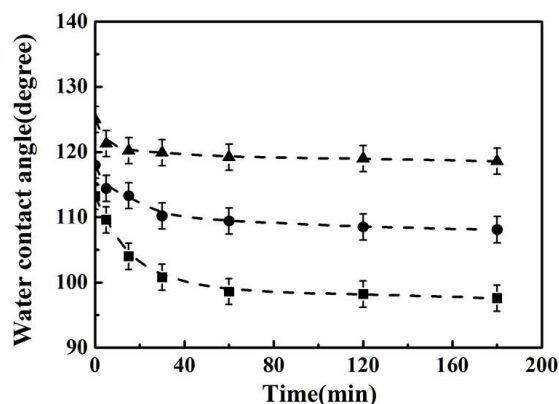


Fig. 2 Time-dependent water contact angles of Au-PMMA<sub>126</sub>-*ec*-FMA<sub>2</sub> (■), Au-PODMA<sub>103</sub>-*ec*-FMA<sub>2</sub> (●) and Au-PMMA<sub>65</sub>-*b*-PODMA<sub>24</sub>-*ec*-FMA<sub>2</sub> (▲) brushes immersed in water at 25°C.

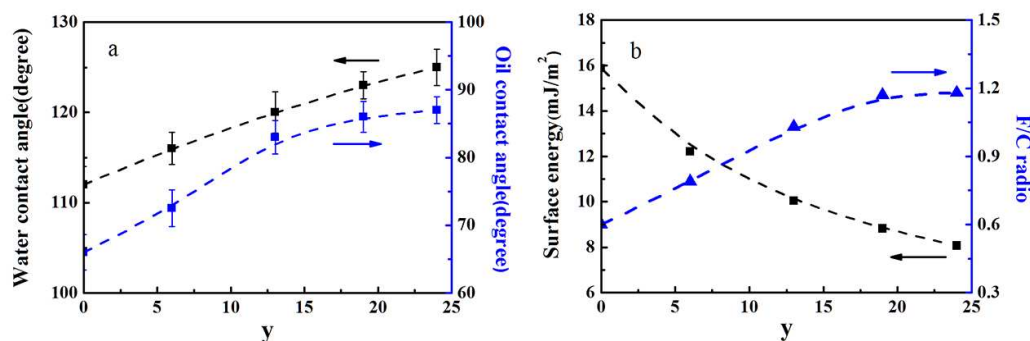


Fig. 3 Water and oil contact angles (a), surface free energy and F/C ratio (b) of Au-PMMA<sub>65</sub>-*b*-PODMA<sub>y</sub>-*ec*-FMA<sub>2</sub> brushes. TOA=30°

Au-PMMA<sub>126</sub>-*ec*-FMA<sub>2</sub> surface and 10° for the Au-PODMA<sub>103</sub>-*ec*-PFMA<sub>2</sub> surface. From these results, the Au-PMMA<sub>65</sub>-*b*-PODMA<sub>24</sub>-*ec*-FMA<sub>2</sub> surface obviously exhibited the best stability and resistance to the polar environments. Therefore, we accordingly designed fluorinated diblock acrylate copolymer brushes to investigate the influence of the length of the PODMA block (y) on their corresponding surface properties and chemical structures.

The water and oil contact angles, surface free energies and F/C ratios of

Au-PMMA<sub>65</sub>-*b*-PODMA<sub>*y*</sub>-*ec*-FMA<sub>2</sub> brushes are presented in Fig. 3. It is apparent that the water contact angle increased from 112° to 125° and the oil contact angle increased noticeably from 66° to 87° as the degree of polymerization of PODMA increased from 0 to 24. The corresponding surface free energy decreased from 15.9 to 8.0 mJ/m<sup>2</sup>, which is close to the critical surface tension ( $\gamma_c$ ) of closely packed trifluoromethyl (-CF<sub>3</sub>) groups (6 mJ/m<sup>2</sup>).<sup>29</sup> The chemical composition and orientation of the perfluorinated alkyls of the topmost surface region were quantitatively analyzed by XPS.<sup>39</sup> The XPS spectra in Fig. S6 (ESI†) shows that the intensities of the F<sub>1s</sub> peaks became noticeably stronger with increasing polymerization degree of PODMA (*y*) namely, with the increasing mass of PFMA in the topmost region. The F/C ratios

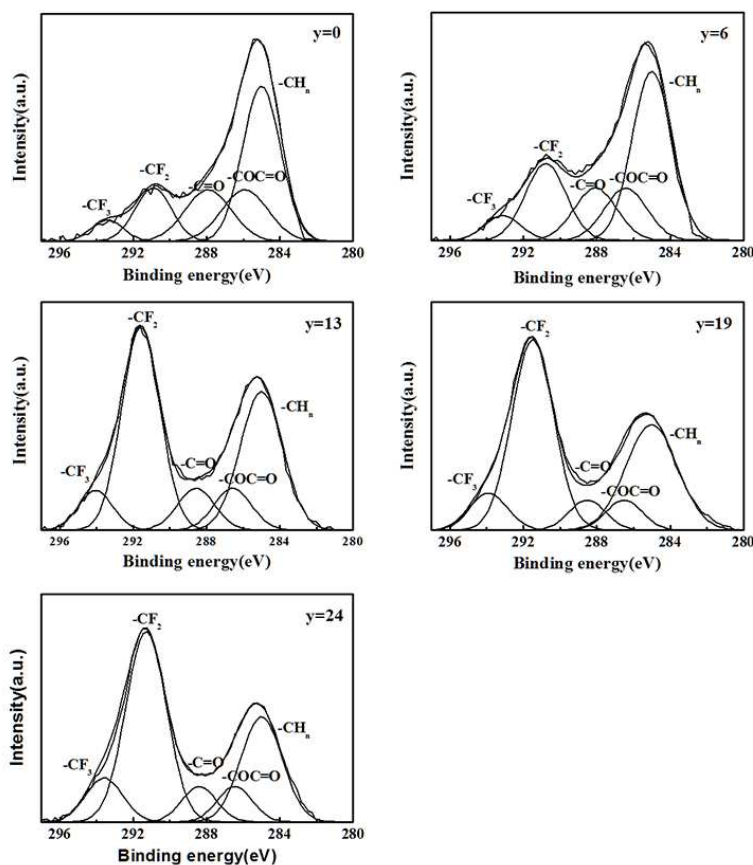


Fig. 4 XPS C<sub>1s</sub> core level spectra of Au-PMMA<sub>65</sub>-*b*-PODMA<sub>*y*</sub>-*ec*-PFMA<sub>2</sub> brushes for various values of *y*, the degree of polymerization of PODMA; TOA=30°

determined from XPS increased from 0.60 to 1.18 as the polymerization degree of

PODMA increased from 0 to 24. These observations demonstrate that the enrichment of fluorinated species in the topmost surface region was due to the increase of PODMA polymerization degree.

To further investigate the orientational state of the perfluorinated end groups at the brushes surface, high-resolution resolved XPS  $C_{1s}$  spectra were recorded. The discrete peaks were assigned to different carbon-based functional groups, and their composition was calculated from the relative peak areas of the individual carbon components. Fig. 4 shows the XPS  $C_{1s}$  core level spectra of the Au-PMMA<sub>65</sub>-*b*-PODMA<sub>*y*</sub>-*b*-PFMA<sub>2</sub> brushes surface for a 30° take-off angle. The spectra were resolved into five Gaussian curve-fitted peaks:  $-CF_3$  at around 294.0 eV,  $-CF_2-$  around 291.5 eV,  $-C=O$  around 288.5 eV,  $-C-O-C=O$  around 286.5 eV, and hydrocarbon ( $-CH_n$ ;  $n = 0-3$ ) around 284.6 eV, from high to low binding energy, respectively. The peak assignments agree well with previously reported values.<sup>74</sup> It was reported that the information about the conformation and packing of the perfluorinated tails could be provided by concentration profiles of these groups and their relative intensity ratios, since the perfluoroalkyl group is composed of the  $CF_3$  head group and a sequence of seven  $CF_2$  groups.<sup>75</sup>

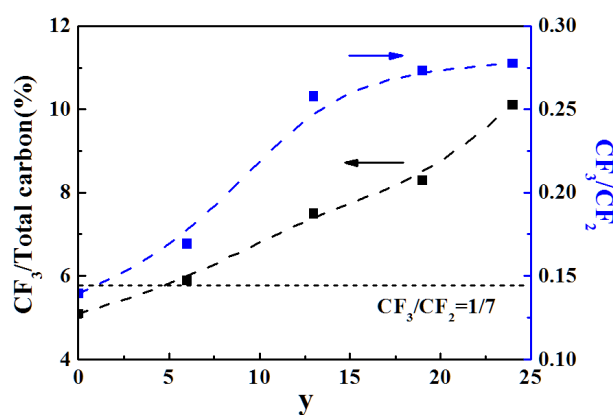


Fig. 5  $CF_3$ /(Total carbon) ratio and  $CF_3/CF_2$  ratio of Au-PMMA<sub>65</sub>-*b*-PODMA<sub>*y*</sub>-*ec*-FMA<sub>2</sub> brushes as a function of *y*, the degree of polymerization of PODMA.

The surface compositions of Au-PMMA<sub>65</sub>-*b*-PODMA<sub>*y*</sub>-*ec*-FMA<sub>2</sub> surfaces are listed in Table S1 (ESI†). Fig. 5 indicates that the  $CF_3$ /(Total carbon) ratio increased

from 5.1 to 10.1, while the values of the  $\text{CF}_3/\text{CF}_2$  ratio increased from 0.14 to 0.27 as  $y$  increased from 0 to 24. Except for the Au-PMMA<sub>129</sub>-*ec*-PFMA<sub>2</sub> brush, the  $\text{CF}_3/\text{CF}_2$  ratios of the other brushes were larger than the theoretical value (0.142). Since the theoretical  $\text{CF}_3/\text{CF}_2$  ratio of this perfluorinated group is 0.142, this value indicated that the brush surface was saturated with perfluorinated groups and all perfluorinated groups was lying flat on the surface.<sup>75,78</sup> When this ratios was above 0.142, this fluorinated groups at the surface are oriented perpendicularly to the surface and a brush with exposed  $-\text{CF}_3$  groups could accordingly be formed.<sup>75</sup> Therefore, compared to the Au-PMMA<sub>129</sub>-*ec*-FMA<sub>2</sub> brush, these results suggest that the introduction of PODMA blocks preceding two FMA units will promote segregation of the perfluorinated groups and the formation of a well-ordered and perpendicularly

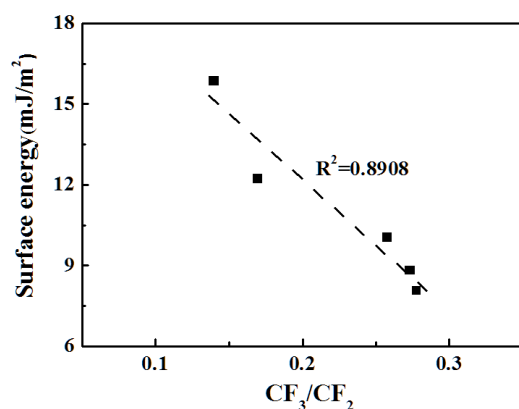


Fig. 6 Surface energy versus  $\text{CF}_3/\text{CF}_2$  ratio for Au-PMMA<sub>65</sub>-*b*-PODMA <sub>$y$</sub> -*ec*-PFMA<sub>2</sub> brushes

oriented structure on the brush surface. This suggestion was also confirmed by the corresponding surface free energies, as shown in Fig. 6. The surface free energies of Au-PMMA<sub>65</sub>-*b*-PODMA <sub>$y$</sub> -*ec*-FMA<sub>2</sub> brushes decrease linearly with the increase of  $\text{CF}_3/\text{CF}_2$  ratios. When the  $\text{CF}_3/\text{CF}_2$  ratio is 0.27, the corresponding surface free energy is 8.07mJ/m<sup>2</sup>, which is close to a surface with a perfectly close-packed crystalline array of  $-\text{CF}_3$  groups.<sup>76</sup>

### 3.3 Role of PODMA Block in Enrichment of Fluorinated Units on the Brush Surface

Both the crystallizability and the flexibility of one of the components of a copolymer are known to affect the segregation of another component with a lower surface free energy.<sup>77,78</sup> The crystallinity of PODMA was considered to be important role in the segregation and the orientation of perfluorinated alkyl groups in the cast films of fluorinated PODMA.<sup>38,39</sup> Since the thicknesses of the Au-PMMA<sub>65</sub>-*b*-PODMA<sub>*y*</sub>-*ec*-PFMA<sub>2</sub> brushes were around 20 nm, it was difficult to use both XRD and DSC techniques to study their crystallinities. Atomic force microscopy (AFM) nanomechanical measurements, such as the recently developed PeakForce quantitative nanomechanics (QNM), have become a straightforward, efficient method for high spatial resolution imaging of material properties by exploiting the Young's modulus changes.<sup>79-81</sup> In order to study the highly-ordered fluorinated groups of polymer brushes, the AFM PeakForce QNM mode, a truly surface sensitive technique, was employed to measure the elastic modulus (E) of the brushes at various temperatures. These results are presented in Fig. 7.

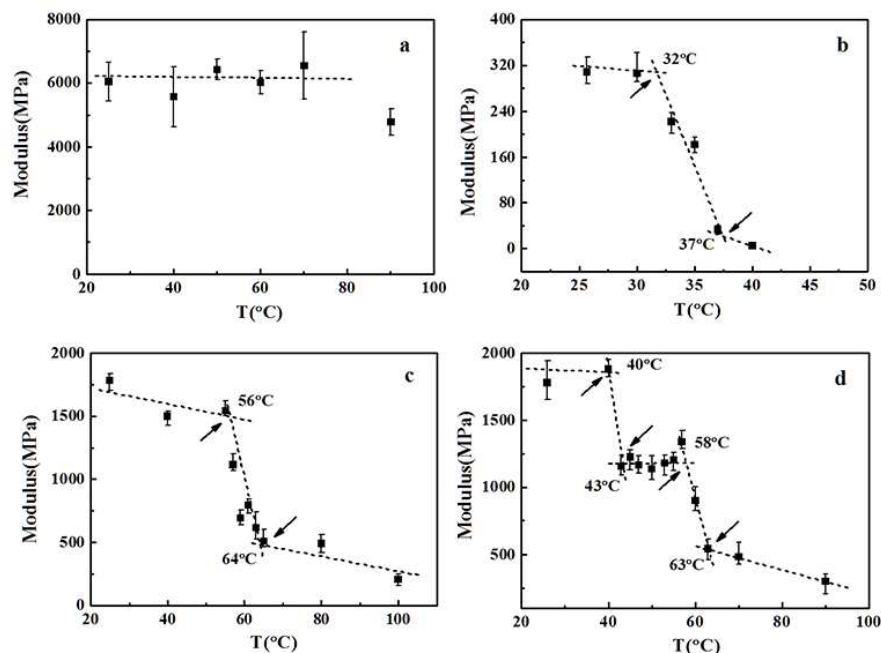


Fig. 7 Elastic modulus versus temperature for various fluorinated polymer brushes. (a) Au-PMMA<sub>126</sub>, (b) Au-PODMA<sub>103</sub>, (c) Au-PMMA<sub>126-ec-FMA<sub>8</sub></sub>, (d) Au-PMMA<sub>65-b-PODMA<sub>24-ec-FMA<sub>2</sub></sub></sub>

Fig. 7(a) shows that the elastic modulus of the Au-PMMA<sub>126</sub> homopolymer brush did not change, staying at around 6 GPa as the temperature increased from room temperature to 70 °C. The elastic modulus of the Au-PODMA<sub>103</sub> homopolymer brush at various temperatures is shown in Fig. 7(b). These results show that there is an abrupt transition from 32°C to 37°C in which the elastic modulus decreases from 300MPa to 50MPa. It was reported previously<sup>38,39</sup> that the melting point temperature of the PODMA crystalline structure in PODMA homopolymer and PMMA-*b*-PODMA diblock copolymer was approximately 35°C. Thus, this transition in Fig.7(b) should be attributed to melting of a crystalline structure formed by the long alkyl chain side group in the PODMA brush. These results indicate that it is reasonable to measure the elastic modulus of polymer brushes at various temperatures. Fig.7(c) shows that the elastic modulus of Au-PMMA<sub>126-ec-FMA<sub>8</sub></sub> brush suddenly decreased from 1.5GPa to 0.5GPa as the temperature increased from 56°C to 64°C. However, the elastic modulus of Au-PMMA<sub>126-ec-FMA<sub>2</sub></sub> brush showed no change within this

temperature range, as shown in Fig. S7(a) (ESI†). It was reported that a peak at around 75 °C, which was attributed to the melting point temperature of a crystalline structure formed by the perfluoroalkyl groups,<sup>82</sup> was also found for FMA end-capped PMMA, PBMA and PMMA-*b*-PBMA films. Thus, this transition in Figure 7(b) should be attributed to melting of a crystalline structure formed by the perfluoroalkyl groups in Au-PMMA<sub>126</sub>-*ec*-FMA<sub>8</sub>.

The change in elastic modulus of the Au-PMMA<sub>65</sub>-*b*-PODMA<sub>24</sub>-*ec*-FMA<sub>2</sub> brush with temperature is shown in Fig. 7(d). Two abrupt transitions are observed within the ranges of 40°C~43°C and 58°C~63°C, respectively. At the same time, the elastic modulus of Au-PMMA<sub>65</sub>-*b*-PODMA<sub>6</sub>-*ec*-FMA<sub>2</sub> (Fig.S7(b), (ESI†)) showed no abrupt transition from 25°C to 70°C. According to the results above, the transitions at 40°C~43°C and 58°C~63°C in Fig.7(d) should be attributed to melting of a crystalline structure formed by the long alkyl chain side group in PODMA and by the perfluoroalkyl groups in the FMA end-capped unit in Au-PMMA<sub>65</sub>-*b*-PODMA<sub>24</sub>-*ec*-FMA<sub>2</sub> brush, respectively. Compared to the results for the Au-PMMA<sub>126</sub>-*ec*-FMA<sub>2</sub> and Au-PMMA<sub>65</sub>-*b*-PODMA<sub>6</sub>-*ec*-FMA<sub>2</sub> brushes, these results suggest that the introduction of PODMA blocks preceding an FMA unit promote segregation of the perfluorinated groups and the formation of a well-ordered and perpendicularly oriented structure on the film surface. In addition, it appears that the formation of a crystalline structure of the PODMA block (relatively long block) is favorable toward the perfluoroalkyl groups in FMA forming a well-organized structure, even if the number of FMA units is low.

As shown in Scheme 2, since the Au-PMMA<sub>65</sub>-*b*-PODMA<sub>24</sub>-*ec*-FMA<sub>2</sub> brush was formed by anchoring the end of the PMMA chain on the Au surface by an Au-S bond, semifluorinated, self-assembled layers at the air-polymer interface are reminiscent of push-me/pull-you structures formed by physical forces. Synergistically, this self-assembly process imparts a higher degree of crystallizability to the second block (PODMA). This structure also enhances the surface segregation of perfluorinated groups and the formation of a well-ordered and perpendicularly oriented structure on the brush surface, which is consistent with both the observed increase in surface

concentration of FMA and  $\text{CF}_3/\text{CF}_2$  ratio with increasing length of the PODMA block. Significantly, the crystallizability of the FMA on the brush surfaces could be observed.

### 3.4. Protein adsorption behavior on Au-PMMA<sub>65</sub>-*b*-PODMA<sub>y</sub>-*ec*-FMA<sub>2</sub> brush surfaces

X-ray photoelectron spectroscopy (XPS) was always used to analyze protein adsorption<sup>83-85</sup> and its detection limit reached  $10 \text{ ng/cm}^2$ .<sup>82</sup> Since no nitrogen atom existed in the polymer brushed in this study, XPS was employed to detect proteins adsorbed on the brush surfaces, using the 400 eV peak for  $\text{N}_{1s}$  as the measurement basis. At the same time, we also evaluated the adsorption of BSA protein conjugated with FTIC on a fluorine end-capped polymer brush by fluorescence microscopy. The relative intensities of the  $\text{N}_{1s}$  XPS peak for polymer brush surfaces with various lengths of the PODMA block are shown in Fig. 8, using fibrinogen as the adsorbed protein. It is clear from these results that there is a dependence of protein adsorption on the length of the PODMA block in the Au-PMMA<sub>65</sub>-*b*-PODMA<sub>y</sub>-*ec*-FMA<sub>2</sub> brush surface. It is evident that the relative intensities of the  $\text{N}_{1s}$  XPS peaks for polymer brush surfaces decreased with increasing length of the PODMA block in the Au-PMMA<sub>65</sub>-*b*-PODMA<sub>y</sub>-*ec*-FMA<sub>2</sub> brushes. Only trace fibrinogen adsorption on the surface of Au-PMMA<sub>65</sub>-*b*-PODMA<sub>y</sub>-*ec*-FMA<sub>2</sub> brush was observed when the degree of polymerization of the PODMA block was 24.

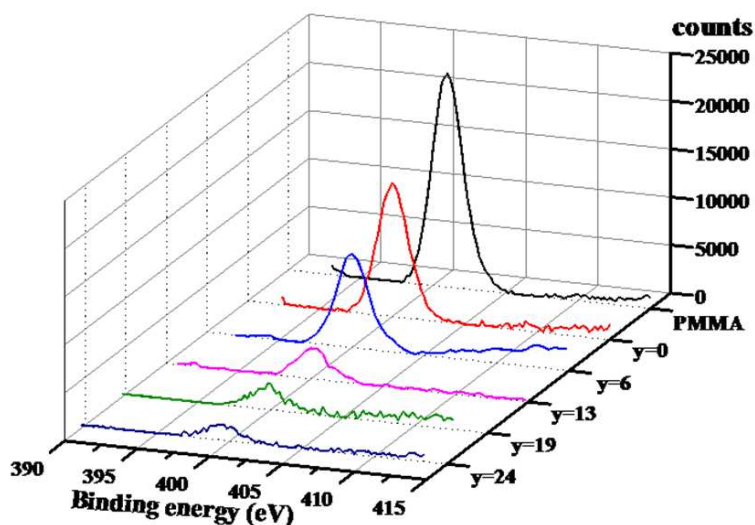


Fig. 8 XPS spectra of  $N_{1s}$  from Au-PMMA<sub>65</sub>-*b*-PODMA<sub>*y*</sub>-*ec*-FMA<sub>2</sub> brush surfaces after fibrinogen adsorption.

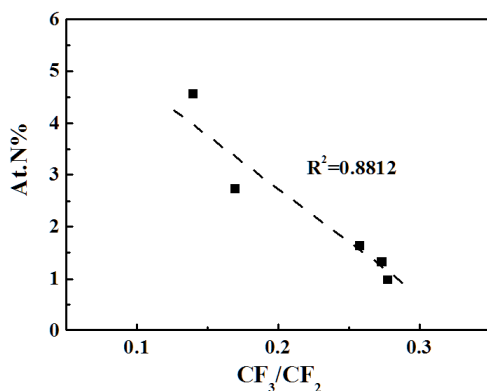


Fig. 9 Atom % of  $N_{1s}$  of adsorbed fibrinogen versus  $CF_3/CF_2$  ratio of Au-PMMA<sub>65</sub>-*b*-PODMA<sub>*y*</sub>-*ec*-FMA<sub>2</sub> brushes

The surface free energy of fluorinated methacrylate polymers depends on the packing of perfluoroalkyl side chains.<sup>38</sup> Herein, it is of great interest for us to determine the relationship between the extent of fibrinogen adsorption and the orientation of the perfluoroalkyl side chains. Fig. 9 depicts the plot of atom % of  $N_{1s}$  of fibrinogen versus  $CF_3/CF_2$  ratio for Au-PMMA<sub>65</sub>-*b*-PODMA<sub>*y*</sub>-*ec*-FMA<sub>2</sub> brushes. The atom % of  $N_{1s}$  adsorbed on the fluorinated brushes is inversely proportional to the

$CF_3/CF_2$  ratio, with a good corresponding linear relationship. Thus, it was apparent that the differences in ordered-packed perfluoroalkyl groups on the brush surfaces are responsible for the observed variations in protein adsorption. When the  $CF_3/CF_2$  ratio is 0.28, there is only trace fibrinogen adsorption, with an atom % of  $N_{1s}$  of 0.69. These results, which were similar to those of solution cast films of poly(*n*-alkyl methacrylate) end-capped with 2-perfluorooctylethyl methacrylate (FMA) reported previously,<sup>47</sup> were further confirmed using fluorescein isothiocyanate-labeled bovine serum albumin (FITC-BSA) as a test protein with fluorescence microscopy (as shown in Fig. 10). According to the corresponding fluorescence micrographs of FITC-BSA adsorbed

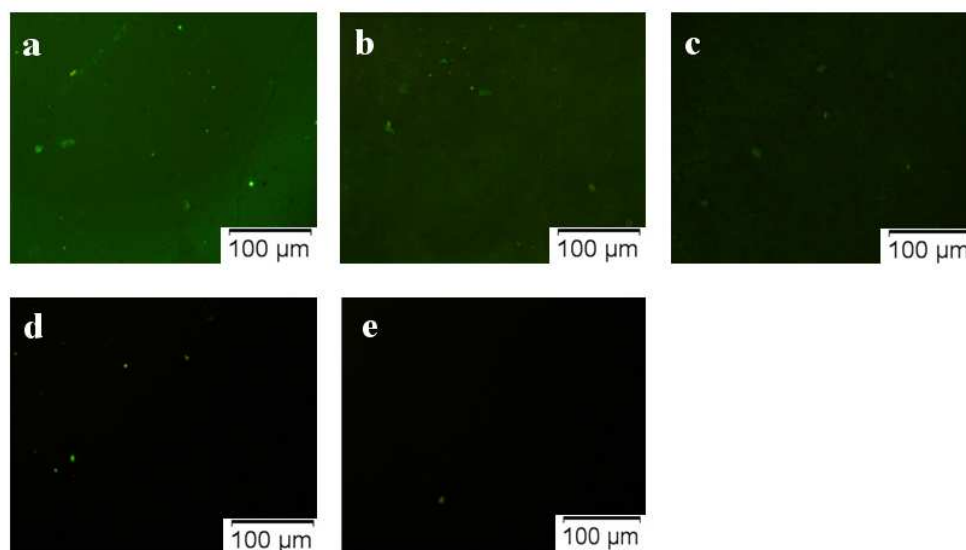


Fig.10 Fluorescence microscopy images for BSA-FITC adsorbed onto Au-PMMA<sub>65</sub>-*b*-PODMA<sub>*y*</sub>-*ec*-FMA<sub>2</sub> brush surfaces. (a) *y*=0 (b) *y*=6 (c) *y*=13 (d) *y*=19 (e) *y*=24.

Scale bar: 100 $\mu$ m

on the surfaces of Au-PMMA<sub>65</sub>-*b*-PODMA<sub>*y*</sub>-*ec*-FMA<sub>2</sub> brushes, BSA adsorption decreased with increasing length of the PODMA block. Only trace BSA adsorption on the surface of Au-PMMA<sub>65</sub>-*b*-PODMA<sub>24</sub>-*ec*-FMA<sub>2</sub> brush was observed, in comparison to obvious adsorption on the surface of the Au-PMMA<sub>65</sub>-*ec*-FMA<sub>2</sub> brush which did not contain a second PODMA block.

The result above showed that the highly close-packed array of perfluoroalkyl side groups correlates positively with improved protein resistance property, which

correspond well with Brady's results,<sup>86</sup> Brady attributed the excellent antifouling performance to the close-packed and oriented trifluoromethyl-terminated groups, which resist diffusion and rearrangement that may potentially lead to infiltration of marine adhesives. Thus, the conclusion could be drawn that protein-resistant property of fluorinated polymer brush correlates with the orientation of the perfluoroalkyl side chains at the surface. Therefore, an optimized coating surface exhibiting unprecedented resistance to proteins should have high enrichment of the fluorine component, and specifically and most importantly, possess a closely-packed perfluoroalkyl groups.

#### 4. CONCLUSIONS

In this paper, fluorinated unit end-capped copolymers with a disulfide group in the chain center were synthesized by atom transfer radical polymerization (ATRP). Acrylate diblock copolymer brushes end-capped with two 2-perfluorooctylethyl methacrylate units Au-PMMA<sub>65</sub>-*b*-PODMA<sub>y</sub>-*ec*-FMA<sub>2</sub> were successfully prepared on Au substrate by a "grafting to" method. These polymer brushes were found to exhibit robust surface segregation of the fluorinated end groups. The increased crystallinity of the second PODMA block plays an important role in the surface segregation and ordering of the fluorinated component at the chain end. The crystallinity of Au-PMMA<sub>65</sub>-*b*-PODMA<sub>y</sub>-*ec*-FMA<sub>2</sub> brush of about 20 nm thickness formed by both the long alkyl chain side group in PODMA and by the perfluoroalkyl groups in FMA respectively, was first observed by the PeakForce quantitative nanomechanics (QNM) technique. A well-ordered and perpendicularly oriented structure of the perfluorinated groups on the brush surface was also confirmed by contact angle measurement, and X-ray photoelectron spectroscopy.

Protein adsorption studies using fibrinogen as a test molecule were undertaken on the various films using XPS. The results show that the adsorbed mass of fibrinogen decreases linearly with increasing order of the structure of the perfluoroalkyl side chains on the surfaces of Au-PMMA<sub>65</sub>-*b*-PODMA<sub>y</sub>-*ec*-PFMA<sub>2</sub> brushes. When the

Au-PMMA<sub>65</sub>-*b*-PODMA<sub>y</sub>-*ec*-PFMA<sub>2</sub> brush surface formed a perfectly close-packed array of -CF<sub>3</sub> groups (y=24), there was only trace fibrinogen adsorption on its surface, which was further confirmed by fluorescein isothiocyanate-labeled bovine serum albumin (FITC-BSA) as a test protein using fluorescence microscopy. This work has demonstrated that the surfaces of polymer brushes with a perfectly close-packed array of perfluoroalkyl groups enhance greatly their protein-resistant performance.

## ACKNOWLEDGMENTS

We are thankful for support from the National Natural Science Foundation of China (NSFC, No.21174134, No.21374104) and the Natural Science Foundation of Zhejiang Province (No. LY13B040005).

## Notes

Department of Chemistry, Key Laboratory of Advanced Textile Materials and Manufacturing Technology of the Education Ministry, Zhejiang Sci-Tech University, Hangzhou 310018, China.

\* Email: [wxinping@yahoo.com](mailto:wxinping@yahoo.com) or [wxinping@zstu.edu.cn](mailto:wxinping@zstu.edu.cn) . Tel/fax: +86-571-8684-3600.

## Supplementary Information

† Electronic Supplementary Information (ESI) available: GPC traces of (S-PMMA<sub>65</sub>-Br)<sub>2</sub> and its cleaved polymer, (Br-PODMA<sub>24</sub>-*b*-PMMA<sub>65</sub>-S)<sub>2</sub>; <sup>1</sup>H NMR spectra of (Br-PODMA<sub>y</sub>-*b*-PMMA<sub>65</sub>-S)<sub>2</sub>; FT-IR spectra of (Br-PMMA<sub>65</sub>-S)<sub>2</sub> and (FMA<sub>n</sub>-*ec*-PMMA<sub>65</sub>-S)<sub>2</sub>; thickness of Au-PMMA<sub>65</sub>-*b*-PODMA<sub>24</sub>-*ec*-PFMA<sub>2</sub> brushes at various rinsing times; XPS spectra of Au-PMMA<sub>65</sub>-*b*-PODMA<sub>y</sub>-*ec*-FMA<sub>2</sub> surfaces; modulus of Au-PMMA<sub>126</sub>-*ec*-FMA<sub>2</sub> and Au-PMMA<sub>65</sub>-*b*-PODMA<sub>6</sub>-*ec*-FMA<sub>2</sub> brushes

at various temperatures; surface composition of Au-PMMA<sub>65</sub>-*b*-PODMA<sub>y</sub>-*ec*-FMA<sub>2</sub> brushes. See DOI: 10.1039/b000000x/

## References

- 1 R. M. Donlan, *Clin. Infect. Dis.*, 2001, **33**, 1387-1392.
- 2 N. Cole, E. B. H. Hume, A. K. Vijay, P. Sankaridurg, N. Kumar, M. D. P. Willcox, *Invest. Ophthalmol. Visual Sci.*, 2010, **51**, 390-395.
- 3 Y. Ohko, Y. Utsumi, C. Niwa, T. Tatsuma, K. Kobayakawa, Y. Satoh, Y. Kubota, A. Fujishima, *J. Biomed. Mater. Res.*, 2001, **58**, 97-101.
- 4 M. D. P. Willcox, E. B. H. Hume, Y. Aliwarga, N. Kumar, N. Cole, *J. Appl. Microbiol.*, 2008, **105**, 1817-1825.
- 5 A. Conte, G. G. Buonocore, A. Bevilacqua, M. Sinigaglia, M. A. Del Nobile, *J. Food Prot.*, 2006, **69**, 866-870.
- 6 E. R. Kenawy, S. D. Worley, R. Broughton, *Biomacromolecules*, 2007, **8**, 1359-1384.
- 7 J. Bozja, J. Sherrill, S. Michielsen, I. Stojiljkovic, *J. Polym. Sci., Part A: Polym. Chem.*, 2003, **41**, 2297-2303.
- 8 K. H. Qi, W. A. Daoud, J. H. Xin, C. L. Mak, W. Z. Tang, W. P. Cheung, *J. Mater. Chem.*, 2006, **16**, 4567-4574.
- 9 N. Wisniewski, M. Reichert, *Colloids Surf. B*, 2000, **18**, 197-219.
- 10 P. S. Asuri, S. Karajanagi, R. S. Kane, J. S. Dordick, *Small*, 2007, **3**, 50-53
- 11 L. D. Chambers, K. R. Stokes, F. C. Walsh, R. J. K. Wood, *Surf. Coat. Technol.*, 2006, **201**, 3642-3652.
- 12 E. Almeida, T. C. Diamantino, O. Desousa, *Prog. Org. Coat.*, 2007, **59**, 2-20.
- 13 R. F. J. Brady, *J. Coat. Technol.*, 2000, **72**, 44-56.
- 14 R. F. J. Brady, I. L. Singer, *Biofouling*, 2000, **15**, 73-81.
- 15 J. R. Saroyan, E. Lindner, C. A. Dooley, H. R. Bleile, *Ind. Eng. Chem. Prod. Res. Dev.*, 1970, **9**, 122-133.
- 16 R. Quintana, M. Gosa, D. Janczewski, E. Kutnyanszky, G. J. Vancso, *Langmuir*, 2013, **29**, 10859-10867.
- 17 S. Chen, L. Li, C. Zhao, J. Zheng, *Polymer*, 2010, **51**, 5283-5293.
- 18 C. Zhao, L. Y. Li, Q. M. Wang, Q. M. Yu, J. Zheng, *Langmuir*, 2011, **27**, 4906-4913.
- 19 R. Konradi, B. Pidhatika, A. Muhlebach, M. Textort, *Langmuir*, 2008, **24**, 613-616.
- 20 D. W. Branch, B. C. Wheeler, G. J. Brewer, D. E. Leckband, *Biomaterials*, 2001, **22**, 1035-1047.
- 21 X. Zhu, H. E. Loo, R. Bai, *J. Membr. Sci.*, 2013, **436**, 47-56.
- 22 M. Anuradha, L. J. William, W. U. Marek, *Macromolecules*, 2009, **42**, 7299-7308.
- 23 A. K. Kinlock, *Adhesion and Adhesives, Science and Technology*; Chapman and Hall: New York, 1987.

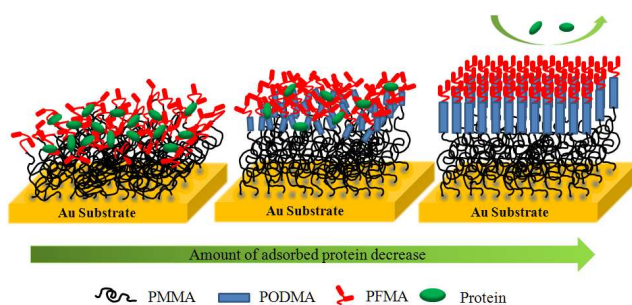
- 
- 24 C. J. Weinman, N. Gunari, S. Krishnan, R. Don, M. Y. Paik, K. E. Sohn, G. C. Walker, E. J. Kramer, D. A. Fischer, C. K. Ober, *Soft Matter*, 2010, **6**, 3237-3243.
- 25 C. S. Gudipati, J. A. Finlay, J. A. Callow, M. E. Callow, K. L. Wooley, *Langmuir*, 2005, **21**, 3044-3053.
- 26 J. Gao, D. A. Mueller, K. L. Wooley, *Journal of Polymer Science Part A: Polymer Chemistry*, 2003, **41**, 3531-3540.
- 27 J. A. Finlay, S. Krishnan, M. E. Callow, R. D. Callow, N. Asgill, K. Wong, E. J. Kramer, C. K. Ober, *Langmuir*, 2008, **24**, 503-510.
- 28 S. Krishnan, R. Ayothi, A. Hexemer, J. A. Finlay, K. E. Sohn, R. Perry, C. K. Ober, E. J. Kramer, M. E. Callow, J. A. Callow, D. A. Fischer, *Langmuir*, 2006, **22**, 5075-5086.
- 29 W. A. Zisman, *ACS Advances in Chemistry*, 1964, **43**, 1-51.
- 30 M. Kanno, H. Kawakami, S. Nagaoka, S. Kubota, *J. Biomed. Mater. Res.*, 2002, **60**, 53-60.
- 31 S. Krishnan, N. Wang, C. K. Ober, J. A. Finlay, M. E. Callow, J. A. Callow, A. Hexemer, K. E. Sohn, E. J. Kramer, D. A. Fischer, *Biomacromolecules*, 2006, **7**, 1449-1462.
- 32 S. H. Baxamusa, K. K. Gleason, *Adv. Funct. Mater.*, 2009, **19**, 3489-3496.
- 33 J. P. Youngblood, L. Andruzzi, C. K. Ober, A. Hexemer, E. J. Kramer, J. A. Callow, J. A. Finlay, M. E. Callow, *Biofouling*, 2003, **19**, 91-98.
- 34 J. G. Wang, G. P. Mao, C. K. Ober, E. Kramer, *Macromolecules*, 1997, **30**, 1906-1914.
- 35 T. Nishino, Y. Urushihara, M. Meguro, K. Nakamae, *J. Colloid Interface Sci.*, 2005, **283**, 533-538.
- 36 Y. Urushihara, T. Nishino, *Langmuir*, 2005, **21**, 2614-2618.
- 37 H. G. Ni, J. Gao, X. H. Li, Y. Y. Hu, D. H. Yan, X. Y. Ye, X. P. Wang, *J. Colloid Interface Sci.*, 2012, **365**, 260-267.
- 38 J. P. Yang, D. X. Yuan, B. Zhou, J. Gao, H. G. Ni, L. Zhang, X. P. Wang, *J. Colloid Interface Sci.*, 2011, **359**, 269-278.
- 39 A. Synytska, D. Appelhans, Z. G. Wang, F. Simon, F. Lehmann, M. Stamm, K. Grundke, *Macromolecules*, 2007, **40**, 297-305.
- 40 D. W. Xue, X. P. Wang, H. G. Ni, W. Zhang, G. Xue, *Langmuir*, 2009, **25**, 2248-2257.
- 41 H. G. Ni, D. W. Xue, X. F. Wang, W. Zhang, X. P. Wang, Z. Q. Shen, *Sci. China, Ser. B.*, 2009, **52**, 203-211.
- 42 X. Y. Ye, B. Zuo, M. Deng, Y. L. Hei, H. G. Ni, X. L. Lu, X. P. Wang, *J. Colloid Interface Sci.*, 2010, **349**, 205-214.
- 43 X. F. Wang, H. G. Ni, D. W. Xue, X. P. Wang, *J. Colloid Interface Sci.*, 2008, **321**, 373-383.
- 44 S. F. Chen, S. Y. Jiang, *Adv. Mater.*, 2008, **20**, 335-338.
- 45 J. Genzer, K. Efimenko, *Science*, 2000, **290**, 2130-2133.
- 46 D. L. Schmidt, R. F. Brady, J. K. Lam, D. C. Schmidt, M. K. Chaudhury, *Langmuir*, 2004, **20**, 2830-2836.
- 47 J. Gao, D. H. Yan, H. G. Ni, L. Wang, Y. H. Yang, X. P. Wang, *J. Colloid Interface Sci.*, 2013, **393**, 361-368.

- 
- 48 J. T. Koberstein, *J. Polym. Sci.: Part B: Polym. Phys.*, 2004, **42**, 2942-2956.
- 49 E. C. Cho, H. Kong, T. B. Oh, K. Cho, *Soft Matter*, 2012, **8**, 11801-11808.
- 50 W. Wu, J. Y. Huang, S. J. Jia, T. Kowalewski, K. Matyjaszewski, *Langmuir*, 2005, **21**, 9721-9727.
- 51 A. K. Nanda, K. Matyjaszewski, *Macromolecules*, 2003, **36**, 1487-1493.
- 52 S. E. Moulton, J. N. Barisci, A. Bath, R. Stella, G. G. Wallace, *Langmuir*, 2005, **21**, 316-322.
- 53 R. R. Shah, D. Merreze, M. Husemann, I. Rees, N. L. Abbott, C. J. Hawker, J. L. Hedrick, *Macromolecules*, 2000, **33**, 597-605.
- 54 B. C. Choi, S. Choi, D. E. Leckband, *Langmuir*, 2013, **29**, 5841-5850.
- 55 Z. Bao, M. L. Bruening, G. L. Baker, *Macromolecules*, 2006, **39**, 5251-5258.
- 56 X. L. Liu, K. Sun, Z. Q. Wu, J. H. Lu, B. Song, W. F. Tong, X. J. Shi, H. Chen, *Langmuir*, 2012, **28**, 9451-9459.
- 57 N. V. Tsarevsky, K. Matyjaszewski, *Macromolecules*, 2002, **35**, 9009-9014.
- 58 W. Van-Camp, F. E. DuPrez, H. Alem, S. Demoustier-Champagne, N. Willet, G. Grancharov, A. S. Duwez, *Eur. Polym. J.*, 2010, **46**, 195-201.
- 59 N. V. Tsarevsky, K. Matyjaszewski, *Macromolecules*, 2005, **38**, 3087-3092.
- 60 F. Montagne, J. P. Maris, R. Pugin, H. Heinzelmann, *Langmuir*, 2009, **25**, 983-991.
- 61 D. K. Owens, R. C. Wendt, *J. Appl. Polym. Sci.*, 1969, **13**, 1741-1747
- 62 R. Bodvik, E. Thormann, L. Karlson, P. M. Claesson, *Phys. Chem. Chem. Phys.*, 2011, **13**, 4260-4268.
- 63 F. Rico, C. M. Su, S. Scheuring, *Nano Lett.*, 2011, **11**, 3983-3986.
- 64 G. Duner, E. Thormann, A. Dedinaite, P. M. Claesson, K. Matyjaszewski, R. D. Tilton, *Soft Matter*, 2012, **8**, 8312-8320.
- 65 H. J. Butt, B. Cappella, M. Kappl, *Surf. Sci. Rep.*, 2005, **59**, 1-152.
- 66 B. Cappella, G. Dietler, *Surf. Sci. Rep.*, 1999, **34**, 5-104.
- 67 R. A. Soldi, A. R. S. Oliveira, R. V. Barbosa, M. A. F. César-Oliveira, *Eur. Polym. J.*, 2007, **43**, 3671-3678.
- 68 X. X. Li, B. Fang, S. Li, P. Wu, Z. W. Han, *Acta Polymer Sinica.*, 2003, **1**, 910-913.
- 69 K. Li, P. P. Wu, Z. W. Han, *Polymer*, 2002, **43**, 4079-4086.
- 70 A. S. Duwez, P. Guillet, C. Colard, J. F. Gohy, C. A. Fustin, *Macromolecules*, 2006, **39**, 2729-2731.
- 71 C. A. Fustin, C. Colard, M. Filali, P. Guillet, A. S. Duwez, M. A. R. Meier, U. S. Schubert, J. F. Gohy, *Langmuir*, 2006, **22**, 6690-6695.
- 72 Z.-L. Wang, J.-T. Xu, B.-Y. Du, Z.-Q. Fan, *J. Colloid Interface Sci.*, 2012, **384**, 29-37.
- 73 Y. Katano, H. Tomono, T. Nakajima, *Macromolecules*, 1994, **27**, 2342-2344.
- 74 T. Nishino, Y. Urushihara, M. Meguro, K. Nakamae, *J. Colloid. Interface. Sci.*, 2004, **279**, 364-369.
- 75 Z. G. Wang, D. Appelhans, A. Synytska, H. Komber, F. Simon, K. Grundke, B. Voit, *Macromolecules.*, 2008, **41**, 8557-8565.
- 76 E. G. Sharfrin, W. A. Zisman, *J. Phys. Chem.*, 1960, **64**, 519-524.

- 
- 77 J. P. Yang, Q. D. Zhao, B. Zhou, H. G. Ni, X. P. Wang, Z. Q. Shen, *Sci. China Ser-B Chem.*, 2009, **52**, 2295-2306.
- 78 R. L. Schmitt, J. J. A. Gardella, J. H. Magill, R. L. Chin, *Polymer*, 1987, **28**, 1462-1466.
- 79 T. J. Young, M. A. Monclus, T. L. Burnett, S. L. Ogin, P. A. Smith, *Meas. Sci. Technol.*, 2011, **22**, 125703.
- 80 K. K. M. Sweers, K. O. Vanderwerf, M. L. Bennink, V. Subramaniam, *ACS Nano*, 2012, **6**, 5952-5960.
- 81 B. Y. Zhao, Y. Song, S. Wanf, B. Dai, L. J. Zhang, Y. M. Dong, J. K. Lu, J. Hu, *Soft Matter*, 2013, **9**, 8837-8843.
- 82 S. Sheiko, E. Lermann, M. Möller, *Langmuir*, 1996, **12**, 4015-4024.
- 83 M. S. Wagner, S. L. McArthur, M. Shen, T. A. Horbett, D. G. Castner, *J. Biomater. Sci. Polym. Ed.*, 2002, **13**, 407-428.
- 84 B.W. Muir, A. Tarasova, T. R. Gengenbach, D. J. Menzies, L. Meagher, F. Rovere, A. Fairbrother, K. M. McLean, P. G. Hartley, *Langmuir*, 2008, **24**, 3828-3835.
- 85 S. Ray, A. G. Shard, *Anal. Chem.*, 2011, **83**, 8659-8666.
- 86 R. F. Brady, S. J. Bonafede, D. L. Schmidt, *Surface Coating International*, 1996, **82**, 582.

**Table of Contents only:****Fabrication of polymer brush surfaces with highly-ordered perfluoroalkyl side groups at the brush end and their antibiofouling properties**

Lin Wang, Xiang Chen, Xinyu Cao, Jianquan Xu, Biao Zuo, Li Zhang, Xinping Wang\*, Juping Yang, Yanqing Yao



The protein-resistant performance was enhanced greatly by constructing polymer brush surface with a perfectly close-packed perfluoroalkyl groups